Synthesis and Electrochemical Properties of V_2O_5 Nanostructures

Ying Wang and Guozhong Cao*

Materials Science & Engineering, University of Washington, Seattle, WA, USA

Keywords: Li^+-intercalation; electrochemical property; Intercalation capacity; V_2O_5 nanostructure.

Abstract. In this seminar, I will present our recent work on the growth and electrochemical properties of single crystalline vanadium pentoxide (V_2O_5) nanorod and Ni-$V_2O_5 \cdot nH_2O$ nanocable arrays. These nanostructures were prepared by solution synthesis and template-based electrodeposition. Processing, morphology, structure and electrochemical properties of these nanostructures will be discussed. These nanostructured electrodes of vanadium pentoxide demonstrate significantly enhanced intercalation capcity and charge/discharge rate compared to the plain film electrodes, due to the high surface area and short diffusion distance offered by nanostructure.

Introduction

Vanadium pentoxide (V_2O_5) is a typical intercalation compound, due to its semiconductivity and layered structure [1]. Accordingly, V_2O_5 has attracted intensive research for many decades to investigate its structure, properties, and technological applications such as lithium batteries and electrochromic displays [2]. The hydrated form of vanadium pentoxide ($V_2O_5 \cdot nH_2O$) has an even higher Li^+-intercalation capacity than its crystalline analogue [3]. However, the intercalation capacity and charge/discharge rate of V_2O_5 are limited by the moderate electrical conductivity (10^{-2} -10^{-3} S/cm)[4] of V_2O_5 and the low diffusion coefficient of Li ions (10^{-12} – 10^{-13} cm^2/s)[5] in V_2O_5. Nanostructured materials possess large surface area (or a large surface to volume ratio) and a short diffusion distance, and thus offer promises to achieve significantly enhanced intercalation capacity, faster intercalation and extraction kinetics, and better cycling fatigue resistance. We have developed three types of nanostructured electrodes: nanorod, nanotube and nanocable arrays of V_2O_5 or $V_2O_5 \cdot nH_2O$, which demonstrated greatly enhanced intercalation capacity at high discharge rates.

Experimental

Single-crystal V_2O_5 nanorod arrays have been grown through template-based method combining three different types of electrodeposition: electrochemical deposition from VO^{2+} solution, surface condensation induced by a pH change from VO_2^+ solution and electrophoretic deposition from V_2O_5 sol, respectively [6 ,7]. Detailed description of the sol electrophoretic deposition process and set-up has been reported previously [8,9]. We have also prepared nanotube arrays of $V_2O_5 \cdot nH_2O$ from similar template-based electrodeposition from VO^{++} solution by using lower voltage and shorter deposition time compared to the conditions for preparing nanorod arrays [10]. Further, Ni-$V_2O_5 \bullet nH_2O$ core-shell nanocable arrays were synthesized with two steps. Ni nanorod arrays were first grown by template-based electrochemical deposition. In the second step, hydrated vanadium pentoxide shell was deposited onto the surface of nickel nanorods through sol electrophoretic deposition. Ni-nanorod arrays have been grown from commercial Ni plating solution NKBP11 (Caswell, Newark, NY) inside polycarbonate templates by electrochemical deposition. The templates used for this study were radiation track-etched hydrophilic PC membrane (Millipore, Bedford, MA) with pore diameters of 200 nm and thickness of 10 μm. The applied voltage was 2.0 V, and the deposition lasted up to 3 hr. Upon

---

* Corresponding author: gzcao@u.washington.edu

the completion of deposition, the samples were dried at 110 °C for 12 hr in air, and the PC membrane was dissolved in methylene chloride subsequently. In the second step, the above Ni nanorod arrays were coated with a thin layer of $V_2O_5 \bullet nH_2O$ by sol electrophoretic deposition. $V_2O_5 \bullet nH_2O$ sols were synthesized using a method reported by Fontenot et al. [11] with V_2O_5 (Alfa Aesar) and 30% H_2O_2 (J.T.Baker) as precursors. Applied voltage was 0.8 V and the deposition lasted up to 15 min. Ni-$V_2O_5 \bullet nH_2O$ core-shell nanocable arrays were characterized by means of scanning electron microscopy (SEM, JEOL JSM-5200), transmission electron microscopy (TEM, Phillips EM420), and X-ray diffractometry (XRD, Philips PW1830). Electrochemical properties of Ni-$V_2O_5 \bullet nH_2O$ nanorod array electrode were investigated by a three-electrode cell. A 1M-$LiClO_4$ solution in propylene carbonate is used as electrolyte, and a Pt mesh is used as counter electrode with $Ag/AgNO_3$ as a reference electrode. Cyclic voltammetry and chronopotentiometric measurements were carried out by potentiostat / galvanostat (EG&G Princeton Applied Research, model 273).

Results and Discussion

Fig. 1 presents SEM and TEM images of single-crystal V_2O_5 nanorod array grown from $VOSO_4$ solution [12]. TEM images and selected area electron diffraction pattern clearly demonstrate the single-crystalline nature of V_2O_5 nanorod with a [010] growth direction. The spacing of the fringes is measured to be 0.207 nm and corresponds well with the spacing of (202) planes at 0.204 nm.

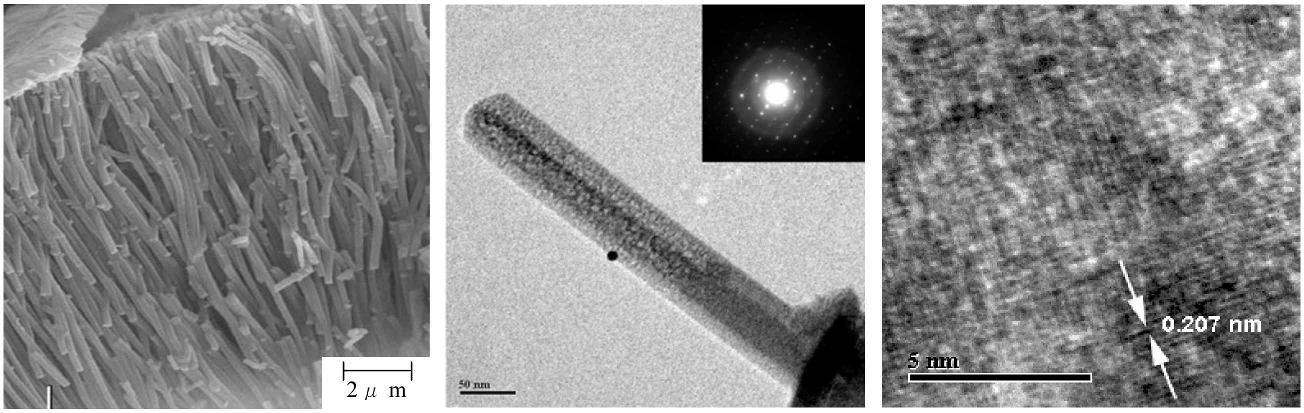

Figure 1. *SEM image of V_2O_5 nanorod arrays (left), high resolution TEM image and electron diffraction pattern (center inset and right) of V_2O_5 nanorod grown from $VOSO_4$ solution.*

Fig. 2 shows typical SEM images of (a) Ni nanorod arrays, and (b) Ni-$V_2O_5 \bullet nH_2O$ core-shell nanocable arrays. Ni nanorod arrays grown by electrochemical deposition have a diameter of ~ 200 nm and stand perpendicular to the substrate. The nanocables after the electrophoretic deposition in $V_2O_5 \bullet nH_2O$ sol have a larger diameter than Ni nanorods, and each nanocable has an independent coating layer with a relatively smooth surface. Fig. 2(c) shows a TEM micrograph of a Ni-$V_2O_5 \bullet nH_2O$ core-shell nanocable. The image of nanocable consists of dark area in the center and light area outside along the axis. This morphology clearly suggests that the nanocable has a layered structure with different composition along the radial, and the dark area is likely to be Ni and the outer area be $V_2O_5 \bullet nH_2O$. Core material is covered completely and uniformly by $V_2O_5 \bullet nH_2O$ shell with a thickness ranging from 30 to 50 nm based on SEM and TEM. Fig. 2(d) is the X-ray diffraction pattern of the $V_2O_5 \bullet nH_2O$ film grown by electrophoretic deposition from the same sol and identical voltage.

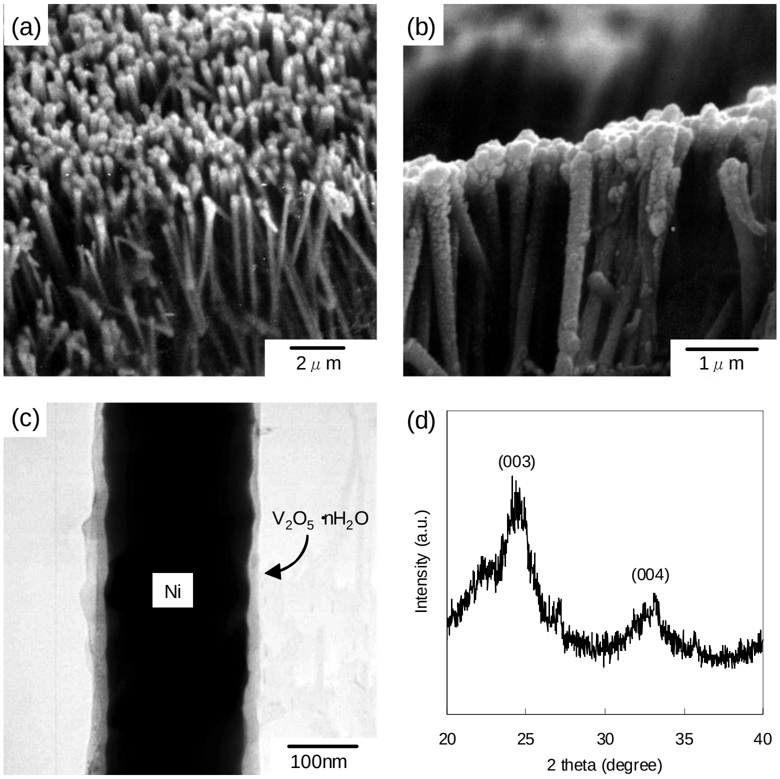

Figure 2. *SEM image of (a) Ni nanorod arrays, and (b) V_2O_5 coated Ni nanorods, (c) TEM micrograph of a Ni-V_2O_5 core-shell nanocable. (d) XRD pattern of V_2O_5 film.*

Fig. 3(a) compares the typical cyclic voltammograms of Ni-V_2O_5•nH_2O nanocable arrays and single crystal V_2O_5 nanorod arrays using a scan rate of 10 mV/sec; the synthesis and electrochemical properties of the latter have been reported in our previous publication [6,12]. The cyclic voltammogram of Ni-V_2O_5•nH_2O nanocable array shows cathodic peaks at -0.4 V and -0.9 V, which are attributed to Li^+ intercalation, and anodic oxidation peaks at 0.0 V and -0.6 V, which are attributed to Li^+ extraction. Single crystalline V_2O_5 nanorod array has cathodic reduction peaks at -0.3 V and -0.9 V, and anodic oxidation peaks at 0.0 V and broad one at -0.6 V. Fig. 3(b) summarizes the Li^+ intercalation capacity as a function of current density of Ni-V_2O_5•nH_2O nanocable arrays, single crystal V_2O_5 nanorod arrays, and sol-gel derived V_2O_5 films. The mass of V_2O_5•nH_2O is calculated based on V_2O_5•nH_2O shell thickness of 40nm (average thickness) and density of 2.87g/cm^3 [13]. Although all three types of structures can achieve high intercalation capacity at a very lower current density, the intercalation capacity of both single crystal V_2O_5 nanorod arrays and sol-gel films decreases rapidly as the current density increases. However, Ni-V_2O_5•nH_2O nanocable arrays retain the high intercalation capacity at very high current densities. For example, in case of current density of 1.6 A/g, core-shell nanocable arrays possess 10 times larger Li^+ intercalation capacity than that of V_2O_5 nanorod arrays and 20 times than that of sol-gel films. Fig. 3(c) shows Ragone plot for Ni-V_2O_5•nH_2O nanocable, V_2O_5 nanorod and sol-gel film. This plot clearly demonstrates that Ni-V_2O_5•nH_2O nanocable arrays have significantly enhanced specific energy (intercalation capacity) and specific power (intercalation kinetics) than those of both single crystal V_2O_5 nanorod arrays and sol-gel V_2O_5 film; the improvement has been at least one order of magnitude under comparable experimental conditions. It should be noted that hydrated vanadium pentoxide possesses higher intercalation capacities than crystalline vanadium [3]. Such significantly improved transport property in Ni-V_2O_5•nH_2O nanocable arrays can be attributed to both short mass transport distance and better electrical conduction. Although V_2O_5 has high capacity of lithium intercalation, it has both low diffusion coefficient of Li^+ in V_2O_5 [5] and low electrical conductivity of V_2O_5 [4]. These two characters limit the intercalation ability of V_2O_5 electrode and explain the fact that in both single crystal nanorod arrays and sol-gel films, a high capacity can only be achieved at a very low current density and the intercalation capacity decreases rapidly as the current density increases. In the case of Ni-V_2O_5•nH_2O core-shell structure, Ni core acts as an electrode, resulting in a relatively large effective electric field applied on the thin V_2O_5•nH_2O layer (shell). In addition, the V_2O_5•nH_2O layer with a thickness of 30-50 nm offers a short diffusion distance for both Li ions and electrons. Our separate results on V_2O_5 nanotube arrays can be found in our other publication [10].

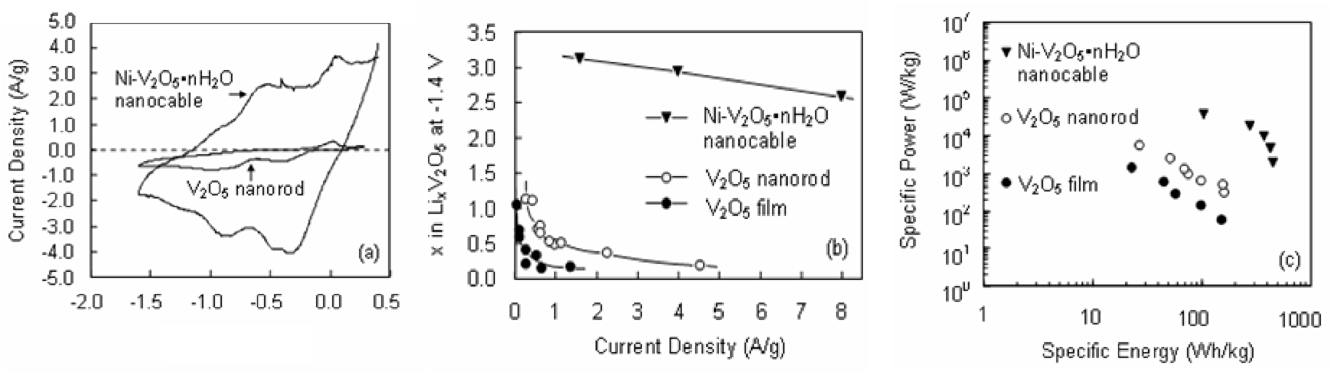

Figure 3. (a) Cyclic voltammograms using a scan rate of 10mV/sec, (b) Relationship between current density and moles of Li intercalated per mole of V_2O_5 calculated from chronopotentiometric measurements and (c) Ragone plot, for Ni-V_2O_5•nH_2O nanocable array, V_2O_5 nanorod array and film.

Summary

Both single-crystal V_2O_5 nanrod arrays and Ni-$V_2O_5 \cdot nH_2O$ core-shell nanocable arrays exhibit significantly improved capacity and charge/discharge rate in comparison with the film electrode. At a current density of 1.6 A/g, Li^+ intercalation capacity of Ni-V_2O_5•nH_2O nanocable arrays is approximately 10 times higher than that of single-crystal V_2O_5 nanorod arrays and 20 times higher than that of sol-gel-derived V_2O_5 film. Both energy density and power density of such nanocable-array electrodes are higher than those of V_2O_5 film electrode by over one order of magnitude. This significant improvement in electrochemical performance of nanostructured vanadium oxide is ascribed to large surface area and short diffusion distance provided by nanostructured $V_2O_5 \cdot nH_2O$.

Acknowledgements: YW wants to acknowledge Ford, JIN and UIF graduate fellowships and this work is supported in part by National Science Foundation (DMI-0455994).

References

[1] H. G. Bachmann, F. R. Ahmend, W. H. Z. Barnes: Kristallorgr. Vol .115 (1961), pp. 110.
[2] K. E. Swider-Lyons, C. T. Love, D. R. Rolison: Solid State Ionics Vol.152-153 (2002), pp. 99.
[3] J. Livage: Chem. Mater. Vol. 3 (1991), pp. 578.
[4] F. Coustier, J. Hill, B.B.Owens, S. Passerini, W. H. Smyrl: J. Electrochem. Soc. Vol. 146 (1999), pp. 1355.
[5] F. Lantelme, A. Mantoux, H. Groult, D. Lincot: J. Electrochem. Soc. Vol. 150 (2003), pp. A1202.
[6] K. Takahashi, S. J. Limmer, Y. Wang, G. Z. Cao: Jpn. J. Appl. Phys. Vol. 44 (2005), pp. 662.
[7] K. Takahashi, Y. Wang, G. Z. Cao: Appl. Phys. Lett. Vol. 86 (2005), pp. 053102.
[8] S. J. Limmer, S. Seraji, M. J. Forbess, Y. Wu, T. P. Chou, C. Nguyen, G.. Z. Cao: Adv. Mater. Vol. 13 (2001), pp. 1269.
[9] S. J. Limmer, S. Seraji, M. J. Forbess, Y. Wu, T. P. Chou, G.. Z. Cao: Adv. Funct. Mater. Vol. 12 (2002), pp. 59.
[10] Y. Wang, K. Takahashi, H. M. Shang, G. Z. Cao: J. Phys. Chem. B Vol. 109 (2005), pp. 3085.
[11] C. J. Fontenot, J. W. Wiench, M. Pruski, G. L. Schrader: J. Phys. Chem. B Vol. 104 (2000), pp. 11622.
[12] K. Takahashi, S. J. Limmer, Y. Wang, G. Z. Cao: J. Phys. Chem. B Vol. 108 (2004), pp. 9795.
[13] Y.J. Liu, J. A. Cowen, T. A. Kaplan, D. C. DeGroot, M. G. Kanatzidis: Chem. Mater. Vol. 7 (1995), pp. 1616.